

Fundus Autofluorescence Lifetimes and Spectral Features of Soft Drusen and Hyperpigmentation in Age-Related Macular Degeneration

Martin Hammer^{1,2}, Rowena Schultz¹, Somar Hasan¹, Lydia Sauer³, Matthias Klemm⁴, Lukas Kreilkamp¹, Lynn Zweifel¹, Regine Augsten¹, and Daniel Meller¹

¹ Department of Ophthalmology, University Hospital Jena, Jena, Germany

² Center for Medical Optics and Photonics, University of Jena, Jena, Germany

³ John A. Moran Eye Center, Salt Lake City, UT, USA

⁴ Technical University Ilmenau, Institute for Biomedical Techniques and Informatics, Ilmenau, Germany

Correspondence: Martin Hammer, University Hospital Jena, Department of Ophthalmology, Am Klinikum 1, 07747, Jena, Germany. e-mail:

martin.hammer@med.uni-jena.de

Received: September 4, 2019

Accepted: February 6, 2020

Published: April 24, 2020

Keywords: age-related macular degeneration; fundus autofluorescence; fluorescence lifetime; drusen; hyperpigmentation

Citation: Hammer M, Schultz R, Hasan S, Sauer L, Klemm M, Kreilkamp L, Zweifel L, Augsten R, Meller D. Fundus autofluorescence lifetimes and spectral features of soft drusen and hyperpigmentation in age-related macular degeneration. *Trans Vis Sci Tech.* 2020;9(5):20. <https://doi.org/10.1167/tvst.9.5.20>

Purpose: To investigate the autofluorescence lifetimes as well as spectral characteristics of soft drusen and retinal hyperpigmentation in age-related macular degeneration (AMD).

Methods: Forty-three eyes with nonexudative AMD were included in this study. Fluorescence lifetime imaging ophthalmoscopy (FLIO), which detects autofluorescence decay over time in the short (SSC) and long (LSC) wavelength channel, was performed. The mean autofluorescence lifetime (τ_m) and the spectral ratio (sr) of autofluorescence emission in the SSC and LSC were recorded and analyzed. In total, 2760 soft drusen and 265 hyperpigmented areas were identified from color fundus photographs and spectral domain optical coherence tomography (SD-OCT) images and superimposed onto their respective AF images. τ_m and sr of these lesions were compared with fundus areas without drusen. For clearly hyperfluorescent drusen, the local differences compared to fundus areas without drusen were determined for lifetimes and sr.

Results: Hyperpigmentation showed significantly longer τ_m (SSC: 341 ± 81 vs. 289 ± 70 ps, $P < 0.001$; LSC: 406 ± 42 vs. 343 ± 42 ps, $P < 0.001$) and higher sr (0.621 ± 0.077 vs. 0.539 ± 0.083 , $P < 0.001$) compared to fundus areas without hyperpigmentation or drusen. No significant difference in τ_m was found between soft drusen and fundus areas without drusen. However, the sr was significantly higher in soft drusen (0.555 ± 0.077 vs. 0.539 ± 0.081 , $P < 0.0005$). Hyperfluorescent drusen showed longer τ_m than surrounding fundus areas without drusen (SSC: 18 ± 42 ps, $P = 0.074$; LSC: 16 ± 29 ps, $P = 0.020$).

Conclusions: FLIO can quantitatively characterize the autofluorescence of the fundus, drusen, and hyperpigmentation in AMD.

Translational Relevance : The experimental FLIO technique was applied in a clinical investigation. As FLIO yields information on molecular changes in AMD, it might support future diagnostics.

Introduction

Age-related macular degeneration (AMD) is a multifactorial disease, affecting the central vision of patients. According to epidemiologic studies, soft drusen and retinal hyperpigmentation are among the main risk factors for AMD progression.¹⁻³ Differ-

ent types of drusen are distinguished based on their location and their appearance in fundus photography and optical coherence tomography (OCT). Soft drusen and basal linear deposits are lipid-rich deposits found between the retinal pigment epithelium (RPE) and Bruch's membrane.⁴ Current theory suggests that lipids and lipoproteins, derived from photoreceptor recycling, are deposited beneath

the RPE. Dietary lipophilic essentials, which are delivered to the RPE and photoreceptors from the choriocapillaris, may also play a role in this deposition. This lipid and lipoprotein accumulation may contribute to AMD pathology by restricting the transport of large molecular complexes⁵ as well as oxygen⁶ from the choroid to the retina. The RPE above deposited drusen may then degenerate by either apoptosis or detachment from its basal membrane, resulting in migration into the retinal space.⁷ This can be visualized in fundus photography as hyperpigmentation or hyper-reflective foci in OCT imaging.⁸

Hyper- and hypofluorescent changes in fundus autofluorescence (FAF) intensity in AMD are well described and classified by different FAF patterns. Bindewald et al.⁹ found that linear hyperfluorescent structures, lacelike patterns, and focal hyper- autofluorescence are associated with hyperpigmentation in fundus photographs. Soft drusen are associated with a patchy FAF pattern and may show normal, hyper-, or hypo-autofluorescence.^{9,10} This was confirmed by histology.¹¹ Conventional FAF imaging, showing autofluorescence intensity only, describes hyper- or hypofluorescent patterns by their morphology but does not allow any investigation of further autofluorescence properties. Fluorescence lifetime imaging ophthalmoscopy (FLIO), on the other hand, was introduced to characterize different fluorophores.^{12,13} Although FLIO shows generally longer autofluorescence lifetimes in AMD compared to age-matched healthy controls, soft drusen did not show longer lifetimes than the surrounding unaffected fundus on average.¹⁴ In contrast, Sauer et al.¹⁵ found slightly longer autofluorescence lifetimes in areas of soft drusen when investigating patients with nonexudative AMD only. Overall, drusen lifetimes show considerable variability and heterogeneity in lifetime patterns.

In this study, we compared autofluorescence lifetimes of soft drusen and hyperpigmentations with those of surrounding fundus areas without drusen in patients with nonexudative AMD. Beyond lifetimes, spectral characteristics of autofluorescence emission were also investigated. The aim of this study was to better understand the diversity of drusen and hyperpigmentations that may be related to the etiology and the progression of AMD.

Methods

Patients and Procedures

In this cross-sectional study, 43 eyes of 39 white patients with nonexudative AMD were enrolled. The mean age was 74.1 ± 7.9 years. The average best-corrected decimal visual acuity was 0.78 ± 0.27 , the

central retinal thickness was $263 \pm 28 \mu\text{m}$, and the intraocular pressure was $17.3 \pm 3.6 \text{ mm Hg}$. A history of choroidal neovascularization as well as geographic atrophy led to exclusion from this study. Other retinal diseases, such as vascular occlusion, diabetic retinopathy, macular telangiectasia type 2, and hereditary retinal dystrophies, were further exclusion criteria. As presence of cataract has been described to alter the FAF lifetimes, patients with mature or incipient cataracts were not included in this study. AMD was graded according to the age-related eye disease study (AREDS) classification by trained ophthalmologists.¹⁶ AMD was graded as stage 2 if drusen greater than 0.042 disk diameters (DD) but smaller than 0.083 DD were found, if the total drusen area was greater than 0.083 DD, or pigment abnormalities were present in the macula. Stage 3 was defined by drusen greater than 0.083 DD, or if the total area of soft drusen was greater than 0.241 DD for indistinct or 0.439 DD for distinct drusen.

The study was approved by the local ethics committee of the University Hospital Jena and it adhered to the tenets of the Declaration of Helsinki. All participants gave written informed consent prior to study inclusion and underwent a full ophthalmologic examination, including best-corrected visual acuity, OCT (Cirrus-OCT; Carl-Zeiss Meditec AG, Jena, Germany) and color fundus photography (Visucam; Carl-Zeiss Meditec AG). Pupils were dilated using tropicamid (Mydriaticum Stulln; Pharma Stulln GmbH, Nabburg, Germany) and phenylephrin-hydrochloride (Neosynephrin-POS 5%; Uraspharm GmbH, Saarbrücken, Germany). After pupil dilation, patients received FLIO imaging. No sodium fluorescein was administered to the cornea or by intravenous injection prior to FLIO investigation.

FLIO Imaging and Data Analysis

Basic principles and laser safety of FLIO are described elsewhere.^{12,17,18} FLIO image capture is based on a picosecond laser diode coupled with a laser-scanning ophthalmoscope (Spectralis; Heidelberg Engineering, Heidelberg, Germany), exciting retinal autofluorescence at 473 nm with a repetition rate of 80 MHz. Fluorescence photons were detected by time-correlated single photon counting (SPC-150; Becker&Hickl GmbH, Berlin, Germany) in a short-wavelength (SSC: 498–560 nm) and a long-wavelength spectral channel (LSC: 560–720 nm). FLIO provides 30-degree field images with a frame rate of nine frames per second and a resolution of 256×256 pixels. Photon histograms over time, describing the autofluorescence decay, were least-square fitted with a series of three exponential functions using the software SPCImage

Table 1. Means \pm Standard Deviations of τ_m in SSC and LSC as Well as the Spectral Ratio sr

Characteristic	τ_m SSC (ps)	τ_m LSC (ps)	sr	N
RPE	289 \pm 70	343 \pm 42	0.539 \pm 0.081	43
Soft drusen	284 \pm 54	337 \pm 34	0.555 \pm 0.076	34
Hyperpigmentations	341 \pm 81	406 \pm 42	0.621 \pm 0.077	23

N is the number of eyes. Values of individual drusen and hyperpigmentations were averaged per eye.

5.5 (Becker&Hickl GmbH). The amplitude-weighted mean decay time τ_m was used for further analysis. The resulting image is color-coded, depicting short lifetimes in red and long lifetimes in blue. In addition, the ratio of photon counts (autofluorescence intensity) in SSC and LSC was calculated per pixel, which is denoted as the spectral ratio (sr).

In total, 2760 soft drusen and 265 hyperpigmentations were manually segmented on color fundus photographs, supported by OCT, using the software GIMP 2.8 (www.gimp.org) to create masks for soft drusen, hyperpigmentations, and unaffected fundus areas. These masks were then transferred to the lifetime τ_m and sr images, which were registered manually to the fundus photographs. Autofluorescence intensity and lifetime images as well as the masks were imported into the software FLIMX, which is documented and freely available for download online under the open-source BSD license (<http://www.flimx.de>). Using FLIMX, τ_m and sr values were averaged per eye across the masks of soft drusen, hyperpigmentations, and across fundus areas without drusen from within the inner and outer ring of the standardized Early Treatment Diabetic Retinopathy Study grid. Additionally, 41 clearly hyperfluorescent soft drusen were segmented from autofluorescence intensity images, and lifetime τ_m and sr of the individual drusen and their immediate surrounding area (three pixels from the drusen margin) were recorded. Drusen size and drusen appearance in fundus photographs (demarcated or diffuse) was also documented.

Statistical Analysis

SPSS 21 (SPSS, Inc., Chicago, IL) was used for all statistical analyses. A *t* test was used to compare means,

with significant difference considered at $P < 0.05$. The Kolmogorov-Smirnov test was used to check for normal distribution. In order to check for contrasts of drusen with their surrounding area, the differences of τ_m and sr were compared to zero. As multiple measurements were taken from patients, a generalized estimating equation was used for comparison of mean values. The Pearson correlation coefficient was calculated in order to check for the association of parameters.

Results

Forty-three eyes of 39 patients were investigated. Six eyes (14%) had AMD stage 2 and 37 eyes (86%) had AMD stage 3. Thirty-four eyes (79%) showed soft drusen. Eighteen eyes (42%) were pseudophakic. Lifetime τ_m averaged over all areas outside of drusen or hyperpigmentations was not significantly different between phakic and pseudophakic eyes (SSC: 300 \pm 62 ps vs. 275 \pm 79 ps, $P = 0.267$; LSC: 338 \pm 40 ps vs. 351 \pm 44 ps, $P = 0.328$). Similarly, spectral ratios were not significantly different either (0.525 \pm 0.083 vs. 0.557 \pm 0.078, $P = 0.203$). Furthermore, none of these parameters showed a significant difference between AREDS stage 2 and stage 3 eyes. Mean values of τ_m and sr are presented in Table 1. A significant or borderline insignificant correlation (P between 0.031 and 0.055) was found for both lifetimes and sr of drusen compared with unaffected fundus areas.

Areas of hyperpigmentation were found in 23 patients. Using a paired *t* test, hyperpigmented areas showed significantly longer autofluorescence lifetimes and the fluorescence emission was shifted toward shorter wavelengths (higher sr) compared to fundus areas without drusen or hyperpigmentations (Table 2). Figure 1 shows an example of hyperpig-

Table 2. Mean \pm Standard Deviations for Differences of Lifetimes ($\Delta\tau_m$) in SSC and LSC as Well as Spectral Ratio Δ sr between Soft Drusen/Hyperpigmentations and Fundus Areas without Drusen or Hyperpigmentations per Eye

Characteristic	$\Delta\tau_m$ SSC (ps)	$\Delta\tau_m$ LSC (ps)	Δ sr	N
Soft drusen	4 \pm 20	3 \pm 14	0.022 \pm 0.075	34
<i>P</i> value	0.228	0.192	<0.001	
Hyperpigmentations	39 \pm 22	49 \pm 31	0.076 \pm 0.036	23
<i>P</i> value	<0.001	<0.001	<0.001	

P values give the significance of differences in paired *t* tests.

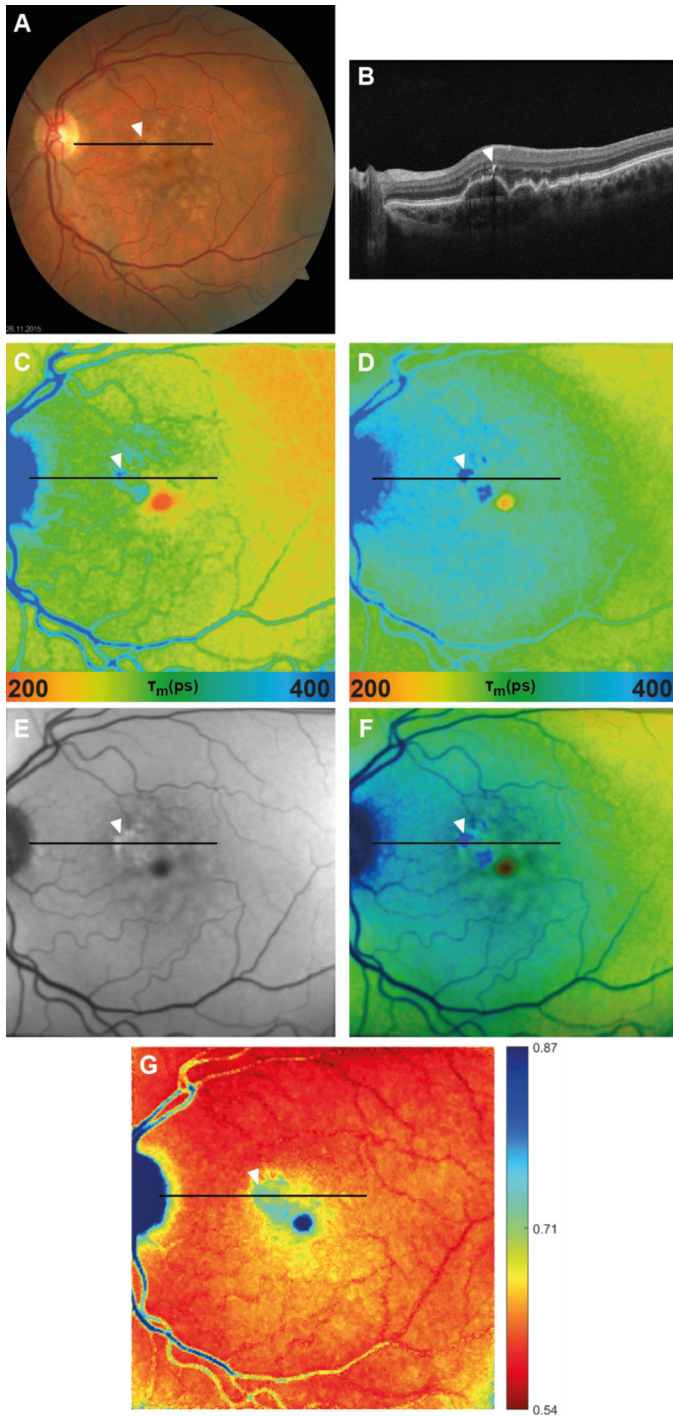


Figure 1. A 63-year-old patient with AMD stage 3 showing hyperfluorescent hyperpigmentations on top of drusen (*white arrowheads*). Fundus photograph (A), with the line indicating the location of the OCT scan (B). OCT section shows RPE migration into the outer retina (*arrowhead*). Autofluorescence lifetime images from the short (498–560 nm, C) and long (560–720 nm, D) wavelength spectral channel show prolonged lifetimes (*arrowheads*). Autofluorescence intensity image (E), overlay of intensity and lifetimes (F), and spectral ratio image (G) are shown as well.

mented spots that were often localized on top of drusen. These presented as hyperreflective foci within the outer retina in OCT images (*arrowhead* in Fig. 1, bottom right). In most cases, areas of long lifetimes in FLIO were larger than hyperpigmentations in fundus photography but smaller than drusen. Furthermore, these eyes often showed spots of considerably prolonged lifetimes in areas of drusen without visible hyperpigmentation.

Thirty-four eyes showed soft drusen. Comparing all drusen with the surrounding fundus, a spectral shift toward shorter emission wavelength was observed with no difference in lifetime found (Table 2). We found eyes with soft drusen that showed longer autofluorescence lifetimes than their surrounding environment (Fig. 2) but also drusen with shorter lifetimes (Fig. 3). In both cases, however, the emission spectra were green-shifted. Figure 2 depicts a case in which the drusen showed long lifetimes, whereas drusenoid pigment epithelial detachments (PEDs), despite being similarly hyperfluorescent, showed short lifetimes.

An analysis focusing on hyperfluorescent drusen only showed that drusen lifetimes were on average 18 ± 42 ps (SSC, $P = 0.074$ in generalized estimating equations) and 16 ± 29 ps (LSC, $P = 0.020$) longer than lifetimes of their immediate surrounding areas. The sr was significantly higher by 0.025 ± 0.049 ($P = 0.003$). Nevertheless, most of the hyperfluorescent drusen were indistinguishable from neighboring fundus regions in FLIO images. Figure 4 shows that longer lifetimes were predominant in drusen with an area less than $70,000 \mu\text{m}^2$. The correlation between drusen size and lifetime, however, was nonsignificant (SSC: $P = 0.060$, LSC: $P = 0.433$). Furthermore, the lifetime differences between drusen and surrounding fundus areas were higher for drusen with demarcated borders in fundus photography than for diffuse drusen (Table 3, Fig. 5). This was significant in the SSC. Demarcated drusen were also smaller and showed a higher green shift of autofluorescence emission than diffuse ones.

Discussion

FLIO lifetimes of drusen in patients with AMD haven been investigated in previous studies. In concordance to our findings, Dysli et al.¹⁴ also found no difference between autofluorescence lifetimes of drusen and their surrounding retina. In contrast, Sauer et al.¹⁵ reported longer lifetimes for soft drusen compared to retina without drusen. However, these authors segmented the drusen from the autofluores-

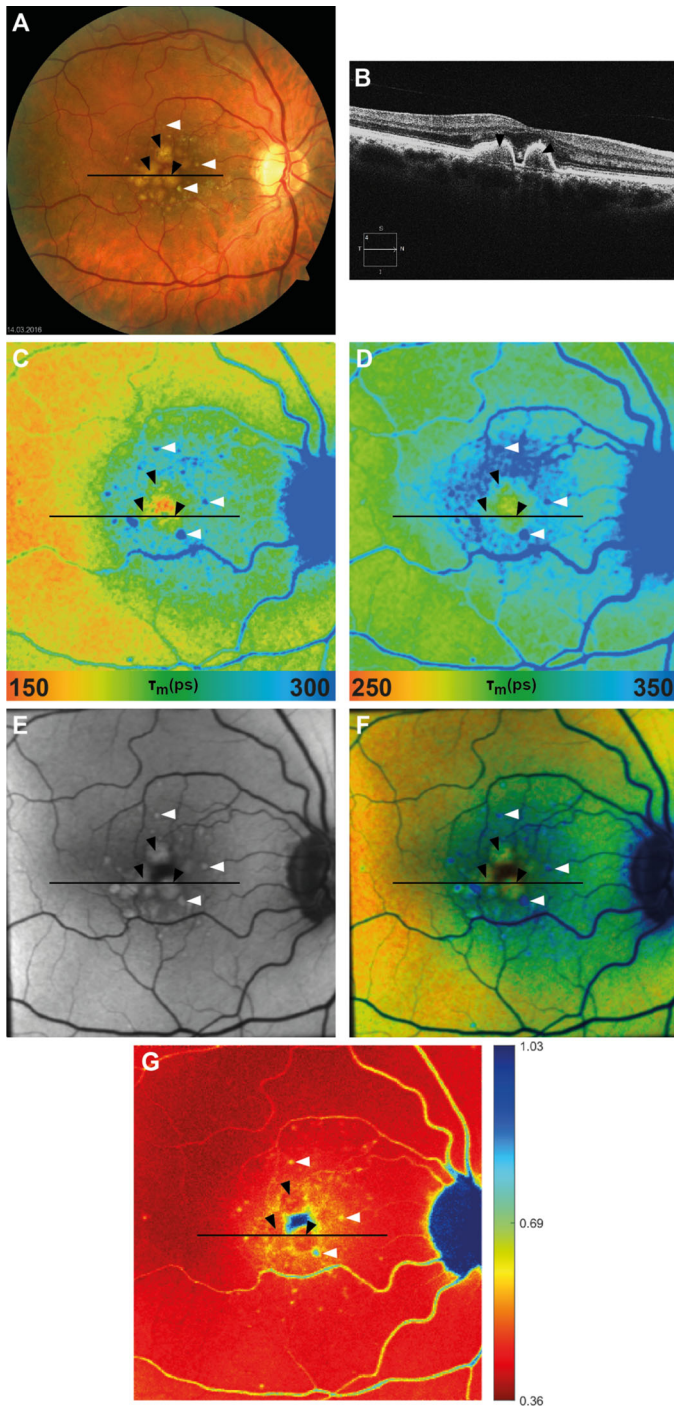


Figure 2. A 66-year-old patient with AMD stage 3 showing hyperfluorescent drusen or drusenoid PEDs (*black arrows*) and drusen (*white arrowheads*). Fundus photograph (A), with the line indicating the location of the OCT scan (B). OCT shows PEDs (*arrowheads*). Autofluorescence lifetime images from the short (498–560 nm, C) and long (560–720 nm, D) wavelength spectral channels show prolonged lifetimes of drusen (*white arrowheads*) and shorter lifetimes for PEDs (*black arrowheads*). Autofluorescence intensity image (E) shows hyperfluorescence of PED as well as drusen, an overlay of intensity and lifetimes (F), and spectral ratio image (G), indicating high sr (green-shifted autofluorescence emission) for drusen but not for PED.

cence images. Thus, their finding is in agreement with our results for hyperfluorescent drusen.

This study presents spectral data of FAF along with autofluorescence lifetimes. Although we did not measure complete spectra, the higher spectral ratio of drusen, compared to their surrounding fundus area, shows a shift of the emission toward shorter wavelengths. This confirms earlier studies that found shorter emission peak wavelengths for sub-RPE deposits, drusen, and Bruch’s membrane compared to RPE in confocal microscopy of histologic sections of donor eyes.^{19,20} Also, widefield epifluorescence microscopy of RPE/Bruch’s membrane flat mounts showed shorter emission wavelengths for drusen than for the RPE.²⁰ Nonnegative tensor factorization²¹ revealed a drusen-specific spectrum.

In our study, about one-third of all soft drusen were hyperfluorescent. Other *in vivo* studies of soft drusen similarly show that there is no good agreement between funduscopically visible drusen and FAF intensity pattern. Whereas Lois et al.²² found hyperfluorescence in macular large soft drusen, Delori et al.²³ reported hyperfluorescent spots, which partly coincided with drusen and often showed a hypofluorescent center, using camera-based imaging techniques. A study by Smith et al.²⁴ resolved the apparent disparity noted above: in early AMD, strong FAF signals colocalized with large soft drusen and hyperpigmentation. This is several times greater than chance, suggesting linked disease processes. In advanced atrophic AMD, higher FAF signals are mostly found adjacent to drusen and geographic atrophy (GA), suggesting a dispersal of drusen-associated lipofuscin, which is a marker of atrophic disease progression. Furthermore, it is known that this “dispersal of lipofuscin” in the case of drusen has a histologic correlate. Considering the anatomy of the ocular fundus, fluorescence contributions from various cellular and extracellular structures have to be taken into account. Since the strongest autofluorescence signal is emitted from lipofuscin within RPE cells, hypofluorescence on top of the druse, eventually along with a hyperfluorescent annulus, may result from a displacement of lipofuscin or gradual degeneration of the RPE.^{23,25} This is also seen on hyperspectral autofluorescence imaging, with attenuation of lipofuscin over the dome of a soft druse and increased lipofuscin where the RPE is draped over the side.²⁰ RPE degranulation and lipofuscin redistribution are also described as an early sign of AMD.²⁶ In the case of GA, increased autofluorescence at the border is now explained by stacking of RPE cells.²⁷

However, histologic investigations also revealed an additional autofluorescence originating from drusen

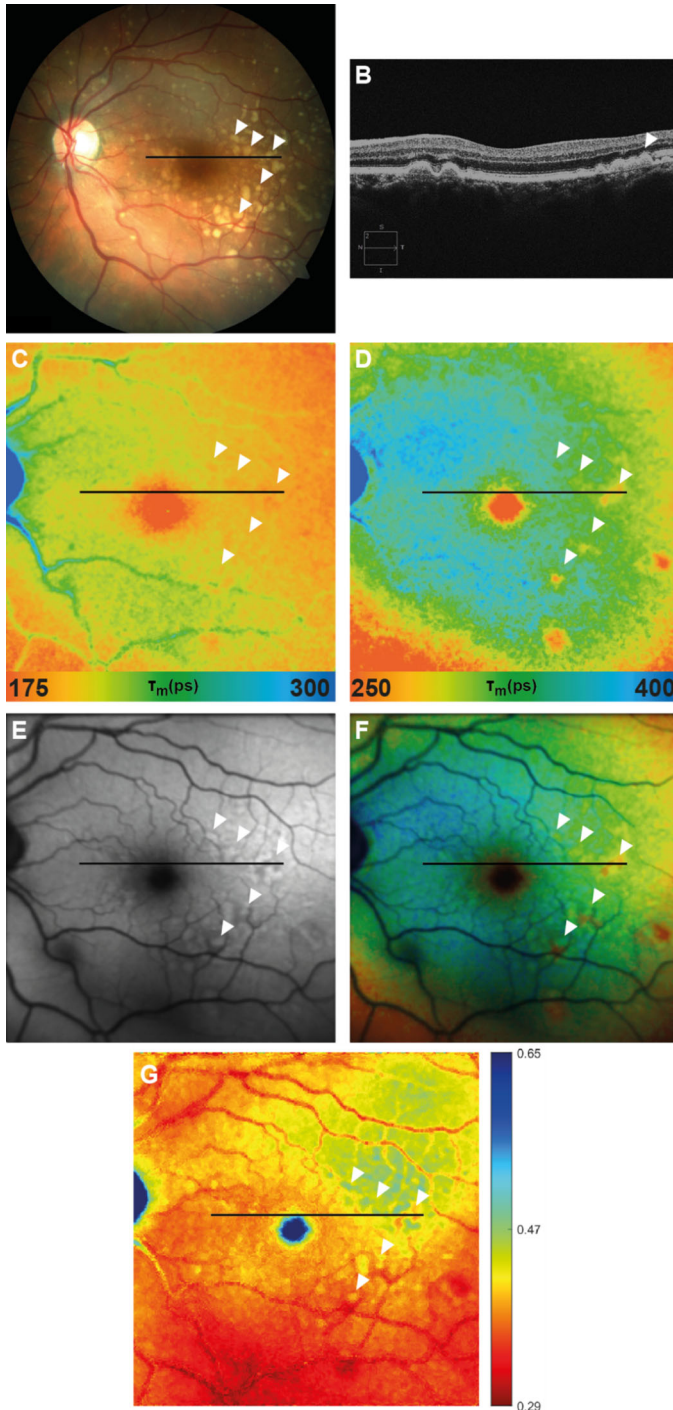


Figure 3. A 65-year-old patient with AMD stage 3 showing hyperfluorescent drusen (*arrowheads*). Fundus photograph (A), with the line indicating the location of the OCT scan (B). OCT shows drusen (*arrowheads*). Autofluorescence lifetime images from the short (498–560 nm, C) and long (560–720 nm, D) wavelength spectral channel show shorter lifetimes for drusen (*arrowheads*) compared to surrounding tissue. Autofluorescence intensity image (E) shows hyperfluorescent drusen, an overlay of intensity and lifetimes (F), and spectral ratio image (G), indicating high sr (green-shifted autofluorescence emission) for drusen.

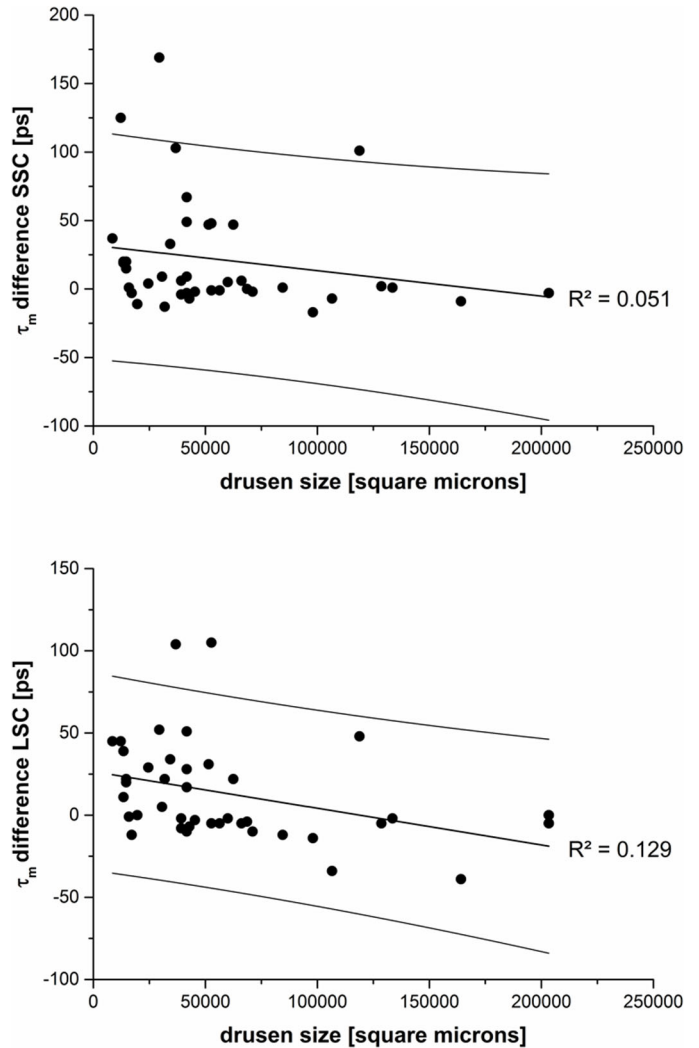


Figure 4. Difference between lifetime τ_m of hyperfluorescent drusen and their immediate surroundings versus drusen area in square microns. Drusen area was recalculated from the pixel size and number in the image. Thus, it holds for the emmetropic eye and does not account for possible individual differences in the axial length.

themselves.^{11,19} Different autofluorescence properties of drusen, RPE, and sub-RPE deposits were found in previous studies of hard and soft drusen as well as basal laminar deposits. Shorter emission wavelengths and longer fluorescence lifetimes were described for sub-RPE deposits.^{11,19,28} This may show up in vivo upon diminished RPE autofluorescence. The effect is possibly stronger for demarcated drusen with steeper borders, although this needs to be investigated further with enhanced contrast OCT images. On the other hand, diffuse drusen and RPE detachment occasionally showed hyperfluorescence as well, mostly occurring without lifetime changes. The origin of this additional autofluorescence is currently not well understood. Although lipofuscin granules were sometimes found in drusen,²⁹ these were too small to explain

Table 3. Means \pm Standard Deviations of Differences between Soft Drusen and Fundus Areas without Drusen for Lifetimes ($\Delta\tau_m$) in SSC and LSC as Well as Spectral Ratio Δsr and Drusen Size Distinguished by Drusen Border (Demarcated or Diffuse)

Characteristic	$\Delta\tau_m$ SSC (ps)	$\Delta\tau_m$ LSC (ps)	Δsr	Size (Pixels)	<i>N</i>
Demarcated	39 \pm 47	32 \pm 27	0.048 \pm 0.052	29.7 \pm 22.6	18
Diffuse	-3 \pm 21	3 \pm 26	0.009 \pm 0.024	65.2 \pm 49.2	17
<i>P</i> value	0.045	0.464	0.001	0.005	

The *P* value gives the asymptotic significance for the comparison of both entities by Mann-Whitney *U* test.

a general hyperfluorescence. Further investigations should address FAF properties of those lesions.

Drusen are known to undergo a cycle of formation and regression. Overall, drusen tend to grow over time, and drusen with a small initial volume are less likely to decrease. Drusen collapse is more likely in large drusen.³⁰ This specifically holds true for drusenoid PEDs.³¹ Differences in autofluorescence lifetimes and *sr* and their relation to drusen size and demarcation, found here, indicate a variable content of fluorescent compounds. Drusen are known to contain apolipoproteins, esterified and unesterified cholesterol, and triglycerides as well as hydroxyapatite.^{4,32–34} Lipid peroxidation may cause an activation of the complement system, RPE cell damage, chronic inflammation, and neovascularization, all contributing to the pathogenesis of AMD.^{4,32} Major constituents are low- and high-density plasma lipoproteins (low-density lipoprotein and high-density lipoprotein), vitamins A and E, lutein from the choroidal circulation,^{35,36} and ApoB and E lipoproteins³⁷ from the RPE side. Unesterified and esterified cholesterol can contribute to drusen and basal linear deposits from the choroid as well as the RPE.³⁸ It might be speculated that the composition of drusen changes over their life cycle, but this has to be proven in longitudinal studies. Anyway, the high variability of autofluorescence lifetimes indicates a chemical diversity and heterogeneity of drusen. This opens questions about the molecular entities responsible for these different lifetimes as well as their role in AMD pathology. However, answers cannot be given from this cross-sectional in vivo study. This would need histologic studies, isolation and analysis of single fluorescent compounds, and longitudinal studies.

Hyperpigmentations are known to be a risk factor for AMD progression to GA.^{39,40} As shown with OCT, such hyperpigmentations are RPE cells that detached from their basal membrane and migrated into the retina.⁴¹ They are known to be hyperfluorescent in a lacelike pattern.^{9,42} Focal hyperpigmentations in AMD have not been investigated with FLIO before. In agreement with literature,^{39,40} in our

study, hyperpigmentations were mostly associated with drusen (PED was excluded from this study). This study is the first to show differences in the autofluorescence properties (longer decay times and shorter emission wavelength) of anteriorly migrated RPE cells compared to RPE attached to Bruch's membrane (Fig. 1). In fundus photography, these lesions appear as dark spots, which could be due to a higher melanin content of those cells. It is, however, questionable whether melanin accounts for changes in the FAF of the hyperpigmented spots. Melanin has been previously described to show a weak autofluorescence with very short decay times.^{43,44} Furthermore, a long-wave emission, which can be excited by near-infrared illumination, is reported for melanin.^{45,46} The autofluorescence of RPE cells predominantly originates from lipofuscin. Lipofuscin granules can be agglomerated with melanosomes, which are subsequently called melano-lipofuscin granules.²⁶ As lipofuscin is a mixture of various lipids, lipoproteins, and retinal-derived molecules, its composition might change upon RPE migration. A consequence of this change may be an alteration of autofluorescence properties. These alterations, however, are poorly understood as the fluorophores of lipofuscin are complex. Chloroform extracts of RPE partially purified 10 fluorescent fractions, but these were never further characterized.⁴⁷ Very recently, hyperspectral characterization of macular fluorophores suggests three main families, but their molecular species is still unknown.²⁰ Although these include multiple bis-retinoids, principally A2E and related compounds, these are found only in the periphery of human eyes and not in the macula.⁴⁸ On the other hand, drusen express inflammatory mediators,^{49,50} which can be chemotactic.^{51,52} These may also change the embedding matrix of fluorophores and, subsequently, alter their lifetimes.

A general prolongation of autofluorescence lifetimes at the posterior pole was found in patients with AMD.^{14,15,53} This raises the question of whether a change in fluorophore composition within the RPE occurs, potentially even before RPE migration begins.

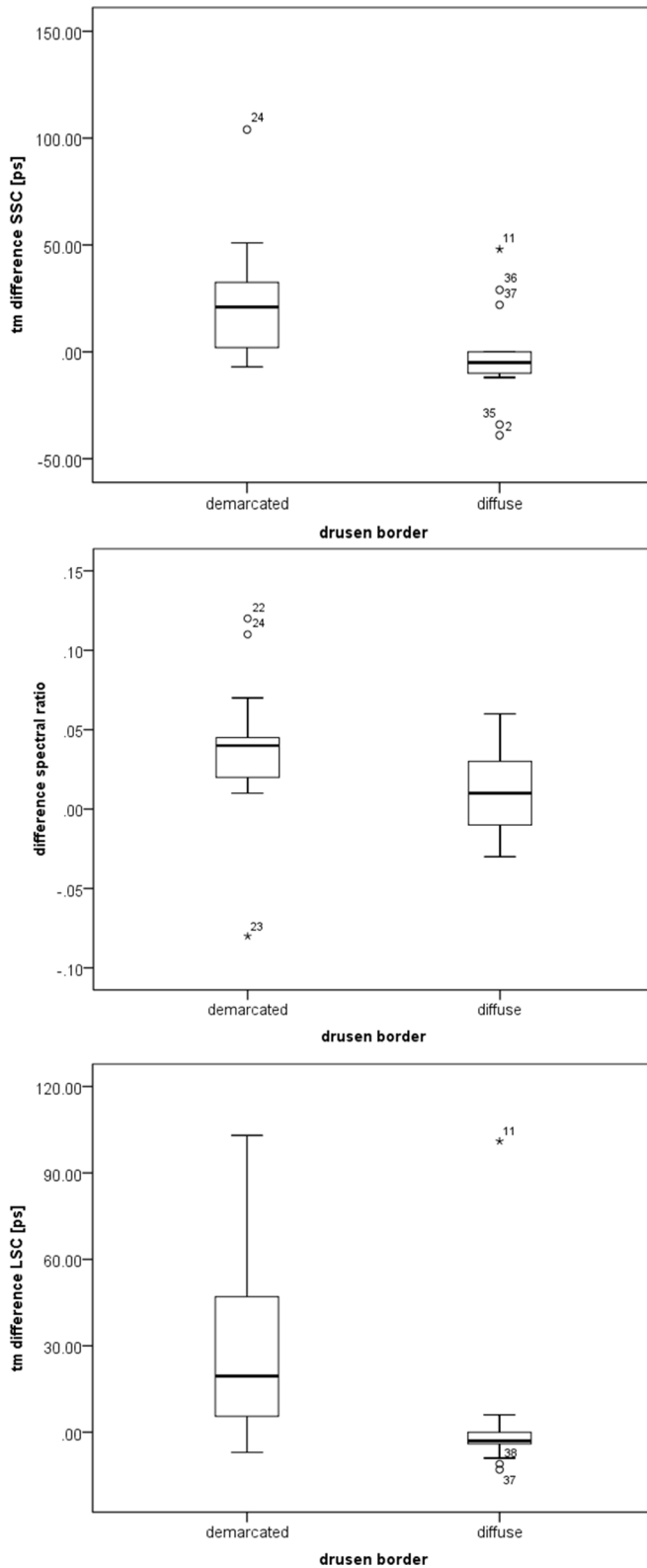


Figure 5. Difference between lifetime τ_m as well as sr of hyperfluorescent drusen and their immediate surroundings versus drusen border.

This possibility is supported by the fact that spots of long lifetimes are usually larger than their corresponding hyperpigmentations seen in fundus photography and that eyes with hyperpigmentation frequently show a focal prolongation of lifetimes at the areas of drusen. If a subsequent development of hyperpigmentation at such lesions would be found in longitudinal studies, new opportunities would arise for FLIO in the early detection of RPE changes and AMD progression. Furthermore, eyes with hyperfluorescent drusen showed spots of prolonged lifetimes in areas of drusen without visible hyperpigmentation. It cannot be stated conclusively whether these spots represent alterations in the RPE or in the drusen. It might be possible that the prolongation of lifetime may result from sub-RPE deposits. Thickening of the RPE–basal lamina band in OCT is observed in AMD, which may support this possibility.⁴¹

Also, retinal autofluorescence should be taken into account. Although the autofluorescence of the retina is considered weak compared to that of the RPE, investigations in porcine eyes, having only minor lipofuscin in their RPE, showed a considerable contribution of inner retinal layers to the total autofluorescence. The retinal autofluorescence showed significantly longer lifetimes than the RPE.⁴⁴ Thus, if AMD progression is associated with RPE redistribution, degranulation, and a loss of lipofuscin,²⁶ the relative contribution of retinal fluorophores as well as fluorophores from sup-RPE deposits to the total autofluorescence lifetime may increase. This could explain the longer lifetimes seen in patients with AMD.¹⁵

This study has several limitations. First, the limited number of patients enrolled in this study has to be mentioned. Nevertheless, statistically significant results were obtained. A higher number of cases in subsequent studies might give further insight into the nature of autofluorescence in drusen and hyperpigmentation. Second, we pooled data from phakic as well as pseudophakic eyes, although we know that lens autofluorescence, despite the confocal scanning technique of FLIO, can contribute to measurements at the fundus. However, no significant difference of FAF lifetimes was found between phakic and pseudophakic patients. Moreover, we investigated the local contrast of autofluorescence lifetimes and sr of drusen or hyperpigmentation with retina without drusen or hyperpigmentation of the same eye. This should greatly eliminate the influence of the lens autofluorescence. Third, a detailed correlation of FLIO data with structural information from the OCT would be desirable. This, however, was precluded by the poor quality of the available OCT scans (Zeiss Cirrus OCT 500). Fourth, this study was restricted to soft drusen only. FLIO

investigation of hard drusen and subretinal drusenoid deposits was excluded because of the limited resolution of FLIO (pixel size $35 \times 35 \mu\text{m}^2$). Finally, our discussion is based on an in vivo observation of parameters, which we believe reflect molecular changes related to AMD. As this is purely noninvasive, we can only speculate on the biochemical background of our observations. Studies on clinicopathologic correlations, using AMD models, as well as combination of our data with that of imaging mass spectrometry,^{54,55} revealing the chemical identity of fluorophores, would be necessary to confirm our speculations.

In conclusion, we found alterations in autofluorescence spectra as well as lifetimes for lesions associated with AMD progression. Whereas hyperpigmentations showed consistently longer autofluorescence lifetimes and shorter emission wavelengths, drusen were virtually indistinguishable from unaffected fundus by their lifetimes. Nevertheless, drusen showed shorter emission wavelengths as well. Moreover, autofluorescence lifetimes of drusen were highly variable, and hyperfluorescent, demarcated drusen tended to show longer fluorescence decays. This study suggests that the autofluorescence emission spectra, rather than autofluorescence lifetimes, might be a more characteristic parameter for drusen identification. Longitudinal observations of autofluorescence lifetimes as well as spectral characteristics, along with quantitative measures of the clinical disease progression, will be critical in order to evaluate the clinical impact of FLIO investigation for drusen and hyperpigmentations.

Acknowledgments

Disclosure: **M. Hammer**, P; **R. Schultz**, None; **S. Hasan**, None; **L. Sauer**, None; **M. Klemm**, None; **L. Kreilkamp**, None; **L. Zweifel**, None; **R. Augsten**, None; **D. Meller**, None

References

- Gass JD. Drusen and disciform macular detachment and degeneration. *Arch Ophthalmol*. 1973;90:206–217.
- Ferris FL, Davis MD, Clemons TE, Lee LY, Chew EY, Lindblad AS. A simplified severity scale for age-related macular degeneration: AREDS Report No. 18. *Arch Ophthalmol Chic*. 2005;123:1570–1574.
- Ferris FL, III, Wilkinson CP, Bird A, et al. Clinical classification of age-related macular degeneration. *Ophthalmology*. 2013;120:844–851.
- Curcio CA, Johnson M, Rudolf M, Huang J-D. The oil spill in ageing Bruch membrane. *Br J Ophthalmol*. 2011;95:1638–1645.
- Cankova Z, Huang JD, Kruth HS, Johnson M. Passage of low-density lipoproteins through Bruch's membrane and choroid. *Exp Eye Res*. 2011;93:947–955.
- Linsenmeier RA, Zhang HF. Retinal oxygen: from animals to humans. *Prog Retin Eye Res*. 2017;58:115–151.
- Zacks DN, Johnson MW. Transretinal pigment migration: an optical coherence tomographic study. *Arch Ophthalmol*. 2004;122:406–408.
- Folgar FA, Chow JH, Farsiu S, et al. Spatial correlation between hyperpigmentary changes on color fundus photography and hyperreflective foci on SDOCT in intermediate AMD. *Invest Ophthalmol Vis Sci*. 2012;53:4626–4633.
- Bindewald A, Bird AC, Dandekar SS, et al. Classification of fundus autofluorescence patterns in early age-related macular disease. *Invest Ophthalmol Vis Sci*. 2005;46:3309–3314.
- Landa G, Rosen RB, Pilavas J, Garcia PM. Drusen characteristics revealed by spectral-domain optical coherence tomography and their corresponding fundus autofluorescence appearance in dry age-related macular degeneration. *Ophthalmic Res*. 2012;47:81–86.
- Schweitzer D, Gaillard ER, Dillon J, et al. Time-resolved autofluorescence imaging of human donor retina tissue from donors with significant extramacular drusen. *Invest Ophthalmol Vis Sci*. 2012;53:3376–3386.
- Schweitzer D, Hammer M, Schweitzer F, et al. In vivo measurement of time-resolved autofluorescence at the human fundus. *J Biomed Opt*. 2004;9:1214–1222.
- Schweitzer D, Schenke S, Hammer M, et al. Towards metabolic mapping of the human retina. *Microsc Res Tech*. 2007;70:410–419.
- Dysli C, Fink R, Wolf S, Zinkernagel MS. Fluorescence lifetimes of drusen in age-related macular degeneration. *Invest Ophthalmol Vis Sci*. 2017;58:4856–4862.
- Sauer L, Gensure RH, Andersen KM, et al. Patterns of fundus autofluorescence lifetimes in eyes of individuals with nonexudative age-related macular degeneration. *Invest Ophthalmol Vis Sci*. 2018;59:AMD65–AMD77.
- AREDS Study Group. The age-related eye disease study system for classifying age-related mac-

- ular degeneration from stereoscopic color fundus photographs: the Age-Related Eye Disease Study Report Number 6. *Am J Ophthalmol*. 2001;132:668–681.
17. Sauer L, Schweitzer D, Ramm L, Augsten R, Hammer M, Peters S. Impact of macular pigment on fundus autofluorescence lifetimes. *Invest Ophthalmol Vis Sci*. 2015;56:4668–4679.
 18. Dysli C, Queller G, Abegg M, et al. Quantitative analysis of fluorescence lifetime measurements of the macula using the fluorescence lifetime imaging ophthalmoscope in healthy subjects. *Invest Ophthalmol Vis Sci*. 2014;55:2106–2113.
 19. Marmorstein AD, Marmorstein LY, Sakaguchi H, Hollyfield JG. Spectral profiling of autofluorescence associated with lipofuscin, Bruch's Membrane, and sub-RPE deposits in normal and AMD eyes. *Invest Ophthalmol Vis Sci*. 2002;43:2435–2441.
 20. Tong Y, Ben Ami T, Hong S, et al. Hyperspectral autofluorescence imaging of drusen and retinal pigment epithelium in donor eyes with age-related macular degeneration. *Retina*. 2016;36(Suppl. 1):S127–S136.
 21. Smith RT, Post R, Johri A, et al. Simultaneous decomposition of multiple hyperspectral data sets: signal recovery of unknown fluorophores in the retinal pigment epithelium. *Biomed Opt Express*. 2014;5:4171–4185.
 22. Lois N, Owens SL, Coco R, Hopkins J, Fitzke FW, Bird AC. Fundus autofluorescence in patients with age-related macular degeneration and high risk of visual loss. *Am J Ophthalmol*. 2002;133:341–349.
 23. Delori FC, Fleckner MR, Goger DG, Weiter JJ, Dorey CK. Autofluorescence distribution associated with drusen in age-related macular degeneration. *Invest Ophthalmol Vis Sci*. 2000;41:496–504.
 24. Smith RT, Chan JK, Busuoiu M, Sivagnanavel V, Bird AC, Chong NV. Autofluorescence characteristics of early, atrophic, and high-risk fellow eyes in age-related macular degeneration. *Invest Ophthalmol Vis Sci*. 2006;47:5495–5504.
 25. Spaide RF, Curcio CA. Drusen characterization with multimodal imaging. *Retina J Ret Vit Dis*. 2010;30:1441–1454.
 26. Ach T, Tolstik E, Messinger JD, Zarubina AV, Heintzmann R, Curcio CA. Lipofuscin redistribution and loss accompanied by cytoskeletal stress in retinal pigment epithelium of eyes with age-related macular degeneration. *Invest Ophthalmol Vis Sci*. 2015;56:3242–3252.
 27. Rudolf M, Vogt SD, Curcio CA, et al. Histologic basis of variations in retinal pigment epithelium autofluorescence in eyes with geographic atrophy. *Ophthalmology*. 2013;120:821–828.
 28. Ben Ami T, Tong Y, Bhuiyan A, et al. Spatial and spectral characterization of human retinal pigment epithelium fluorophore families by ex vivo hyperspectral autofluorescence imaging. *Transl Vis Sci Technol*. 2016;5:5.
 29. Rossberger S, Ach T, Best G, Cremer C, Heintzmann R, Dithmar S. High-resolution imaging of autofluorescent particles within drusen using structured illumination microscopy. *Br J Ophthalmol*. 2013;97:518–523.
 30. Yehoshua Z, Wang F, Rosenfeld PJ, Penha FM, Feuer WJ, Gregori G. Natural history of drusen morphology in age-related macular degeneration using spectral domain optical coherence tomography. *Ophthalmology*. 2011;118:2434–2441.
 31. Balaratnasingam C, Yannuzzi LA, Curcio CA, et al. Associations between retinal pigment epithelium and drusen volume changes during the life-cycle of large drusenoid pigment epithelial detachments. *Invest Ophthalmol Vis Sci*. 2016;57:5479–5489.
 32. Handa JT, Cano M, Wang L, Datta S, Liu T. Lipids, oxidized lipids, oxidation-specific epitopes, and age-related macular degeneration. *Biochim Biophys Acta*. 2017;1862:430–440.
 33. Thompson RB, Reffatto V, Bundy JG, et al. Identification of hydroxyapatite spherules provides new insight into subretinal pigment epithelial deposit formation in the aging eye. *Proc Natl Acad Sci U S A*. 2015;112:1565–1570.
 34. Kishan AU, Modjtahedi BS, Martins EN, Modjtahedi SP, Morse LS. Lipids and age-related macular degeneration. *Surv Ophthalmol*. 2011;56:195–213.
 35. Loane E, Nolan JM, O'Donovan O, Bhosale P, Bernstein PS, Beatty S. Transport and retinal capture of lutein and zeaxanthin with reference to age-related macular degeneration. *Surv Ophthalmol*. 2008;53:68–81.
 36. Tserentsoodol N, Sztein J, Campos M, et al. Uptake of cholesterol by the retina occurs primarily via a low density lipoprotein receptor-mediated process. *Mol Vis*. 2006;12:1306–1318.
 37. Wang L, Li CM, Rudolf M, et al. Lipoprotein particles of intraocular origin in human Bruch membrane: an unusual lipid profile. *Invest Ophthalmol Vis Sci*. 2009;50:870–877.
 38. Curcio CA, Millican CL, Bailey T, Kruth HS. Accumulation of cholesterol with age in human Bruch's membrane. *Invest Ophthalmol Vis Sci*. 2001;42:265–274.
 39. Ouyang Y, Heussen FM, Hariri A, Keane PA, Sadda SR. Optical coherence tomography-based

- observation of the natural history of drusenoid lesion in eyes with dry age-related macular degeneration. *Ophthalmology*. 2013;120:2656–2665.
40. Ho J, Witkin AJ, Liu J, et al. Documentation of intraretinal retinal pigment epithelium migration via high-speed ultrahigh-resolution optical coherence tomography. *Ophthalmology*. 2011;118:687–693.
 41. Curcio CA, Zanzottera EC, Ach T, Balaratnasingam C, Freund KB. Activated retinal pigment epithelium, an optical coherence tomography biomarker for progression in age-related macular degeneration. *Invest Ophthalmol Vis Sci*. 2017;58:BIO211–BIO226.
 42. Einbock W, Moessner A, Schnurrbusch UE, Holz FG, Wolf S. Changes in fundus autofluorescence in patients with age-related maculopathy. Correlation to visual function: a prospective study. *Graefes Arch Clin Exp Ophthalmol*. 2005;243:300–305.
 43. Ehlers A, Riemann I, Stark M, König K. Multiphoton fluorescence lifetime imaging of human hair. *Microsc Res Tech*. 2007;70:154–161.
 44. Hammer M, Sauer L, Klemm M, Peters S, Schultz R, Haueisen J. Fundus autofluorescence beyond lipofuscin: lesson learned from ex vivo fluorescence lifetime imaging in porcine eyes. *Biomed Opt Express*. 2018;9:3078–3091.
 45. Keilhauer CN, Delori FC. Near-infrared autofluorescence imaging of the fundus: visualization of ocular melanin. *Invest Ophthalmol Vis Sci*. 2006;47:3556–3564.
 46. Miura M, Makita S, Sugiyama S, et al. Evaluation of intraretinal migration of retinal pigment epithelial cells in age-related macular degeneration using polarimetric imaging. *Sci Rep*. 2017;7:3150.
 47. Eldred GE, Katz ML. Fluorophores of the human retinal pigment epithelium: separation and spectral characterization. *Exp Eye Res*. 1988;47:71–86.
 48. Ablonczy Z, Higbee D, Anderson DM, et al. Lack of correlation between the spatial distribution of A2E and lipofuscin fluorescence in the human retinal pigment epithelium. *Invest Ophthalmol Vis Sci*. 2013;54:5535–5542.
 49. Pikuleva IA, Curcio CA. Cholesterol in the retina: the best is yet to come. *Prog Retin Eye Res*. 2014;41:64–89.
 50. Anderson DH, Mullins RF, Hageman GS, Johnson LV. A role for local inflammation in the formation of drusen in the aging eye. *Am J Ophthalmol*. 2002;134:411–431.
 51. Hogg PA, Grierson I, Hiscott P. Direct comparison of the migration of three cell types involved in epiretinal membrane formation. *Invest Ophthalmol Vis Sci*. 2002;43:2749–2757.
 52. Jin M, He S, Worpel V, Ryan SJ, Hinton DR. Promotion of adhesion and migration of RPE cells to provisional extracellular matrices by TNF- α . *Invest Ophthalmol Vis Sci*. 2000;41:4324–4332.
 53. Dysli C, Wolf S, Zinkernagel MS. Autofluorescence lifetimes in geographic atrophy in patients with age-related macular degeneration. *Invest Ophthalmol Vis Sci*. 2016;57:2479–2487.
 54. Ablonczy Z, Smith N, Anderson DM, et al. The utilization of fluorescence to identify the components of lipofuscin by imaging mass spectrometry. *Proteomics*. 2014;14:936–944.
 55. Anderson DM, Ablonczy Z, Koutalos Y, et al. High resolution MALDI imaging mass spectrometry of retinal tissue lipids. *J Am Soc Mass Spectrom*. 2014;25:1394–1403.